

201971: gold-bearing grains, Hillside gold prospect

(Kelly Group, East Pilbara Terrane)

Sample type	Gold-bearing grains
Specimens	Two specimens comprising three grains
Total weight	0.2 g
Sample location	Hillside gold prospect, about 52 km west-northwest of Nullagine
Coordinates	MGA zone 50, 775150E 7600480N
Datum	GDA94
1:250 000 map sheet	MARBLE BAR (SF 50-8)
1:100 000 map sheet	SPLIT ROCK (2854)
Tenement	E 45/4685
Collector	Macarthur Minerals



Location and sampling

The sample was provided by Macarthur Minerals in October 2018. It was collected at the Hillside gold prospect in the East Pilbara Terrane. The sample comprises two gold-bearing grains collected from debris in a drainage channel (specimen A; Fig. 1a) and one grain from Au- and Fe-rich chalcedony rocks (specimen B; Fig. 1b) in a nearby quartz reef (Macarthur Minerals, 2018, written comm., 30 October).

Geological context

The Hillside gold prospect is located about 1.3 km west of the Coongan fault system, which is inferred to be a bounding structure to a central graben (Ferguson and Ruddock, 2001). The local bedrock comprises massive to locally pyroxene–spinel-textured, pillowed komatiitic metabasalt of the 3350–3335 Ma Euro Basalt (Hickman, 2021b) of the 3350–3315 Ma Kelly Group (Hickman, 2021c), which is part of the Kelly Large Igneous Province (Hickman, 2021a, 2013; GSWA, 2014).

Several gold prospects (Corboy, Corboy Southeast, Edelweiss and Stubbs) are located 5–6 km north from the Hillside prospect and about 0.5 – 1.3 km west of the Coongan fault system (Bagas et al., 2004). A grab sample from Corboy assayed 33.7 g/t Au, and drilling at Edelweiss intersected gold–pyrite–chalcopyrite mineralization grading 12.3 g/t Au over 5.2 m. These gold deposits are hosted by a thick sequence of high-Mg metabasalt of the Euro Basalt, and are spatially associated with north-northeasterly striking quartz veins (Ferguson and Ruddock, 2001; Bagas et al., 2004).

The nearest regolith landform is an alluvial–fluvial unit comprising unconsolidated gravel, sand, silt and clay in active, but poorly defined, drainage channels on a floodplain. The present-day drainage locally dissects residual or relict, variably silicified, massive, nodular, and cavernous calcrete (GSWA, 2014).

Methodology

The specimens were photographed and weighed, their overall morphology and external features, such as colour, roundness, surface relief, coatings, mineral inclusions and mineral assemblages, were recorded using visual morphometry. The raw surfaces of the samples were analysed using scanning electron microscopy with energy-dispersive X-ray spectroscopy (SEM-EDS). The specimens were mounted in epoxy resin and polished to expose their microstructure and inclusions for examination using reflected-light microscopy and SEM-EDS. Gold microchemistry was determined by laser ablation inductively coupled plasma mass spectrometry (LA-ICP-MS), calibrated against certified gold reference materials (CRM; Murray, 2009). The specimens were ablated in duplicate or triplicate along 0.5 mm-long traverses and average values calculated for elements present in the CRM. Gold surfaces were repolished after laser ablation, etched with aqua regia, and internal structures examined using reflected-light microscopy. Details of these methods are described in Hancock and Beardsmore (2020).

Morphology

Specimen A consists of two grains with dimensions $6 \times 3 \times 2$ mm and $4 \times 3 \times 3$ mm (Fig. 1a). Gold forms an irregular cement around Fe-oxide minerals (grain 1) or is intergrown with anhedral crystals of translucent quartz (grain 2).

Specimen B is a single grain, with dimensions $3 \times 3 \times 2$ mm (Fig. 1b), and consists of gold interspersed with grey quartz (chalcedony) and Fe-oxide minerals. Gold projections are slightly rounded.

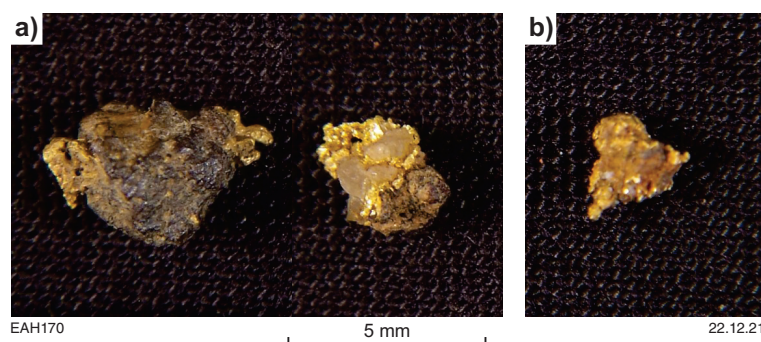


Figure 1. Three gold grains comprise sample 201971: gold-bearing grains, Hillside gold prospect: a) specimen A; b) specimen B

SEM-EDS analysis of raw surfaces

Most of the gold in specimen A exhibits stepped growth features with dissolution triangles on the steps, and partly damaged (rounded) surfaces where gold projects beyond the general margin of the specimen. Flakes, nanoclusters and small crystals of gold are disseminated in patches of Al–Si–Fe-oxide minerals and Mg-rich clays (Fig. 2a).

Gold in specimen B is common as flakes, spherules and clusters disseminated in a Fe–Si–Mg-rich matrix (Fig. 2b).

Optical microscopy of polished surfaces

Gold in specimen A is intergrown with porous, spongiform goethite and rounded quartz grains (Fig. 3a).

Specimen B comprises a mixture of massive irregular gold with rounded projecting edges, and porous goethite and quartz. Some goethite grains are encrusted with very small gold particles (Fig. 3b).

SEM-EDS analysis of polished surfaces

Massive gold in specimen A contains 3.0 – 3.5% Ag, and inclusions of quartz, Fe-oxide minerals, chlorite, and albite. A small amount of pure gold (Ag-free) is disseminated in the matrix of Fe-oxide minerals, clay, albite and chlorite (Fig. 4a).

Massive gold in specimen B contains about 3% Ag, and rounded inclusions of quartz. A mixture of chalcedonic silica, zoned Fe-oxide minerals and very small gold particles mantles the outer rim of massive gold (Fig. 4b). The zonation in Fe-oxide minerals reflects variations in Si and Al content.

LA-ICP-MS analysis

Analyses consistently detected Ag, Cu and Hg within the gold grains, in concentrations higher than the instrumental detection limit, and probably occurring as limited solid solutions in the gold. Other trace elements were detected only sporadically in low (sub-ppm) concentrations, possibly occurring in micro- and nano-inclusions.

The gold specimens contain low concentrations of Ag (3–4%), moderate Cu (400–550 ppm), and relatively high Hg (860–1670 ppm) (Table 1). Elevated concentrations of many elements in specimen B (Table 2) most likely result from partial ablation of regolith materials and/or inclusions.

Acid etching

The internal fabrics of massive gold in both specimens are polycrystalline, and exhibit variable degrees of deformation.

Gold in specimen A shows partial recrystallization of a twinned fabric that has angular, irregular boundaries and several curved twinned planes. Smaller gold grains are rounded, and exhibit deformation-induced polysynthetic twinning and intergranular Ag-depleted veinlets up to 20 µm wide (Fig. 5a).

Gold in specimen B exhibits a strongly deformed, recrystallized fabric with broken and curved crystal boundaries, and transformed incoherent polysynthetic and simple twin planes (Fig. 5b).

Interpretation

All three gold grains possess similar physical and chemical characteristics, indicative of minimal transportation from their primary source. These grains were most likely derived from the same local source as the majority of those comprising sample 201970 (Hancock et al., 2022).

Specimen B of this sample and specimen C of sample 201970 have similar physical and chemical characteristics that typify primary gold mineralization in the area.

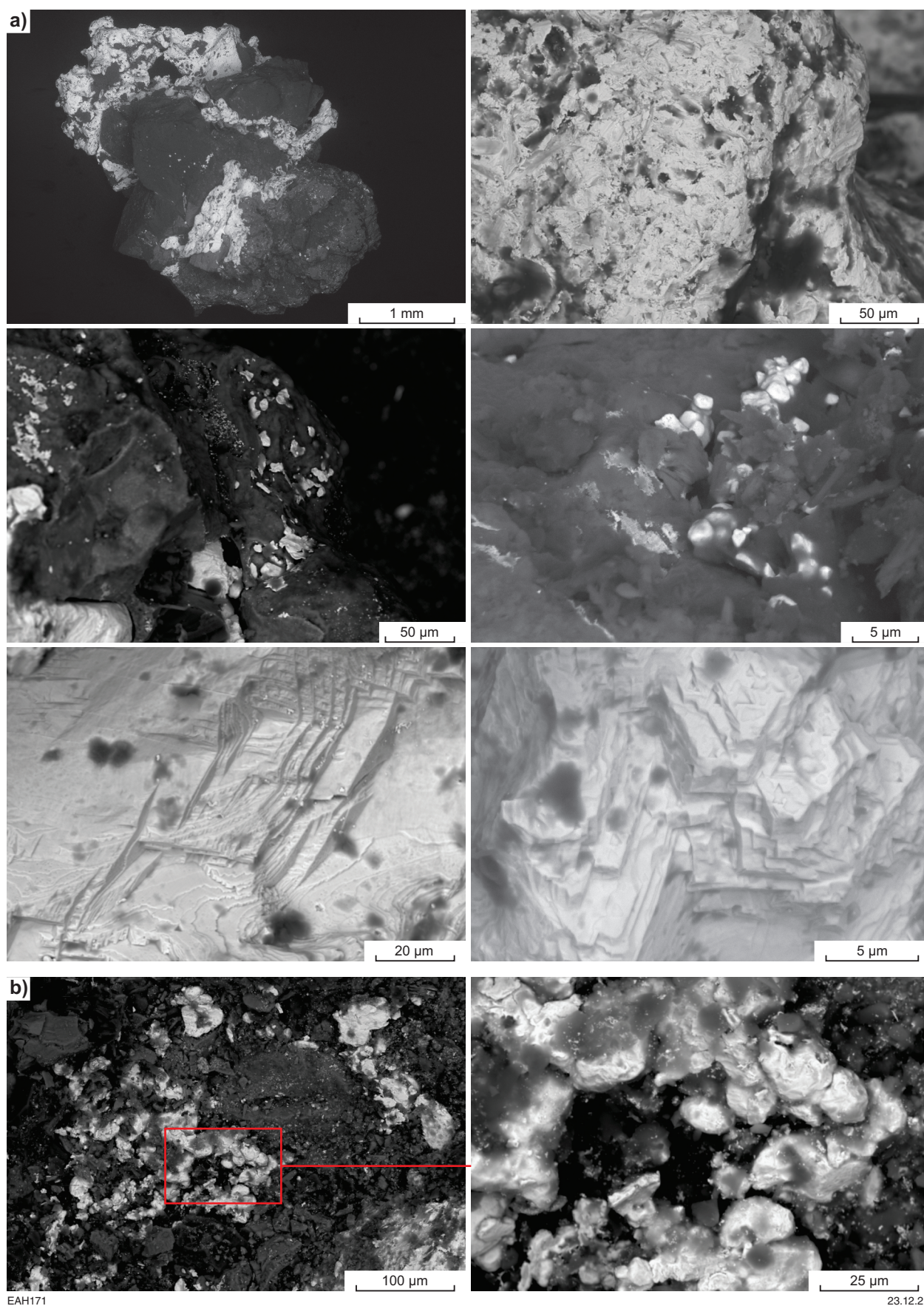


Figure 2. Backscattered electron (BSE) images of sample 201971: gold-bearing grains, Hillside gold prospect: a) specimen A; b) specimen B

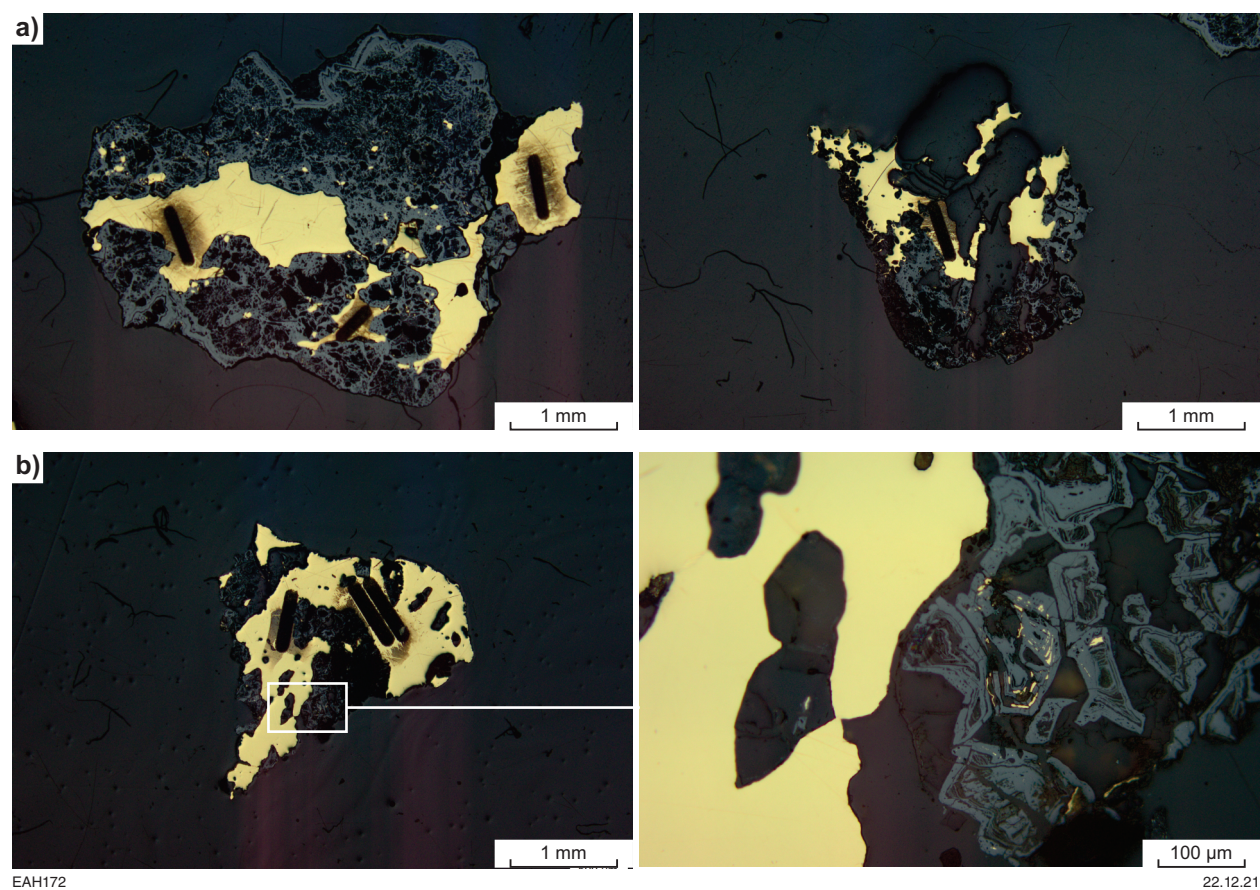


Figure 3. Reflected light photomicrographs of polished surface of sample 201971: gold-bearing grains, Hillside gold prospect: a) specimen A; b) specimen B. Dark elongate lines are laser ablation tracks produced during LA-ICP-MS analyses

Table 1. LA-ICP-MS data for selected elements in sample 201971: gold-bearing grains, Hillside prospect

Specimen	Ag (%)	Cu (ppm)	Hg (ppm)	Minor elements
A	3.2, 3.4, 3.5	387, 487, 547	1480, 1641, 1667	Mg , Pb
B	3.7, 4.0, 4.0	492, 500, 524	857, 933, 1011	Mg, Ti, Ni, Zn, As, Se, Sb, Pb

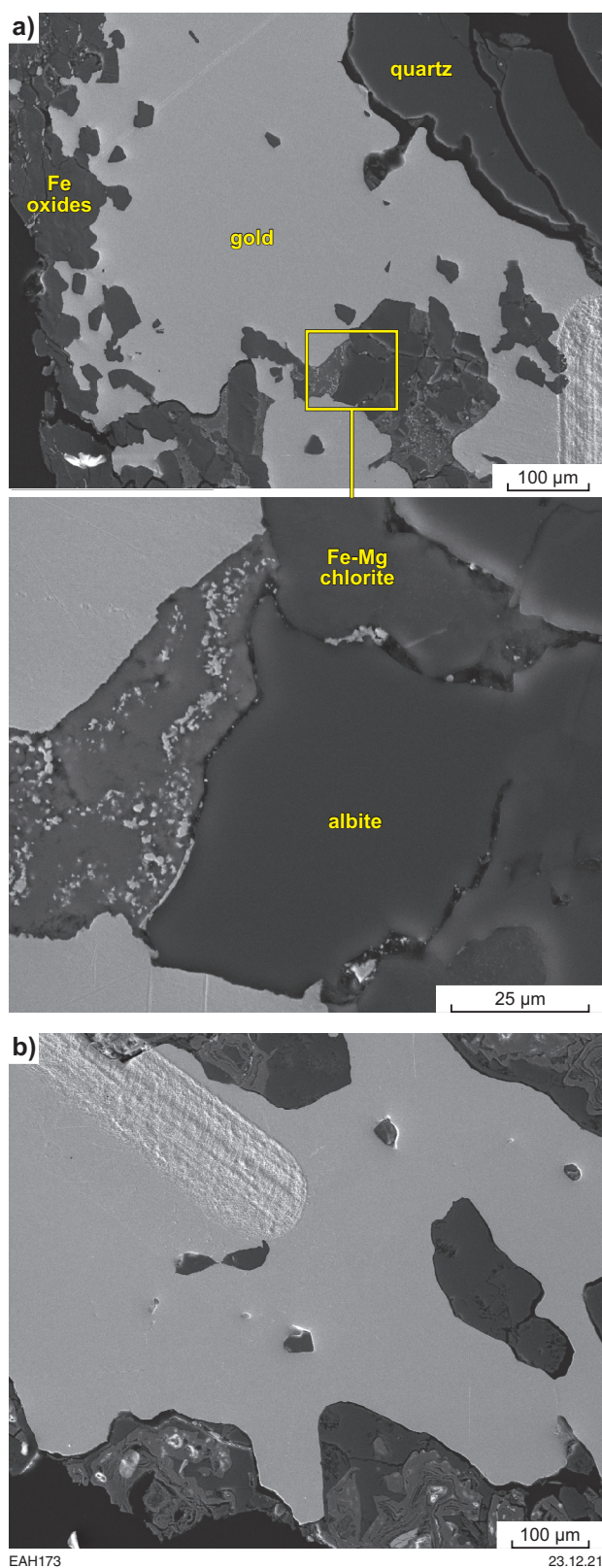


Figure 4. Secondary electron images of selected areas of polished surface of sample 201971: gold-bearing grains, Hillside prospect: a) specimen A; b) specimen B

Table 2. LA-ICP-MS compositional data for sample 201971: gold-bearing grains, Hillside prospect

Specimen and laser ablation track	Unit	⁷ Li	⁹ Be	¹¹ B	²³ Na	²⁵ Mg	²⁷ Al	²⁹ Si	⁴⁴ Ca	⁴⁵ Sc	⁴⁹ Ti	⁵¹ V	⁵³ Cr	⁵⁵ Mn	⁵⁷ Fe	⁵⁹ Co	⁶⁰ Ni	⁶⁵ Cu
A-1	cps					77	583			18	2	13	35	92	583	16	8	47863
A-2	cps					28	302				5		2			4	7	60248
A-3	cps		2			79	33				6	4	8		10	3	3	67750
B-1	cps	559	2		10950	33	461				5	2	19				6	64834
B-2	cps					447	7061				10	37		98	768	11	9	60854
B-3	cps		282	5982	41528	60946	667954	116796	4907	3779	736	59743	117	169078	940743	11777	5691	61949
A-1	ppm					0.92					0.04						0.08	387
A-2	ppm					0.34					0.11						0.07	487
A-3	ppm					0.95					0.12						0.03	547
B-1	ppm					0.40					0.10						0.06	524
B-2	ppm					5.35					0.21						0.09	492
B-3	ppm					730					16.10						58	500

Specimen and laser ablation track	Unit	⁶⁶ Zn	⁶⁹ Ga	⁷² Ge	⁷⁵ As	⁸² Se	⁸⁵ Rb	⁸⁸ Sr	⁸⁹ Y	⁹⁰ Zr	⁹³ Nb	⁹⁸ Mo	¹⁰¹ Ru	¹⁰³ Rh	¹⁰⁸ Pd	¹⁰⁹ Ag	¹¹¹ Cd	¹¹⁵ In
A-1	cps	3		6	8			4			3			3	8	7239541	79	2
A-2	cps	4		4				4			4	1		1	7	7004456	101	
A-3	cps	4						5						2	6	6666085	87	1
B-1	cps							6					1	2	13	7648890	160	2
B-2	cps	4		4	2	1	2	6	7				1	1	15	8168757	151	1
B-3	cps	6652	381	4258	4776	15	99	1365	7195	142	19	63			8	8150442	129	6
A-1	ppm	0.03			0.10									0.006	0.06	35126		0.004
A-2	ppm	0.04												0.002	0.05	33986		
A-3	ppm	0.05												0.004	0.04	32344		0.002
B-1	ppm													0.004	0.10	37113		0.003
B-2	ppm	0.05			0.02	0.08								0.002	0.11	39635		0.002
B-3	ppm	77			58	1.20									0.06	39546		0.011

Specimen and laser ablation track	Unit	¹²⁰ Sn	¹²¹ Sb	¹²⁶ Te	¹³³ Cs	¹³⁸ Ba	¹³⁹ La	¹⁴⁰ Ce	¹⁴¹ Pr	¹⁴⁵ Nd	¹⁵¹ Eu	¹⁵⁷ Gd	¹⁵⁹ Tb	¹⁶² Dy	¹⁶⁵ Ho	¹⁶⁷ Er	¹⁶⁹ Tm	¹⁷² Yb
A-1	cps		11	213		5		3		1						1		
A-2	cps	18	33		1	2												
A-3	cps	31	13	5		1			2						2		1	
B-1	cps	4	15	1	4	3				1		1						
B-2	cps	20	20		4	2	2	2		3		2						
B-3	cps	12	892	32	18	755	461	5041	284	161	212	167	248	420	397	233	157	218
A-1	ppm		0.04	3.91														
A-2	ppm	0.08	0.13															
A-3	ppm	0.14	0.05	0.08														
B-1	ppm	0.02	0.06	0.02														
B-2	ppm	0.09	0.08															
B-3	ppm	0.05	3.47	0.59														

Specimen and laser ablation track	Unit	¹⁷⁵ Lu	¹⁷⁸ Hf	¹⁸¹ Ta	¹⁸² W	¹⁸⁵ Re	¹⁸⁹ Os	¹⁹³ Ir	¹⁹⁵ Pt	²⁰² Hg	²⁰⁵ Tl	²⁰⁸ Pb	²⁰⁹ Bi	²³² Th	²³⁸ U
A-1	cps				1				1	429185	5	1317	49	2	2
A-2	cps									475810		7	8	2	1
A-3	cps							1		483364	2	6	5	2	
B-1	cps	2	2							248536	2		1		
B-2	cps									270504		2	3	1	
B-3	cps	143	3	4	13				2	293046		538	49	49	384
A-1	ppm								0.014	1480		4.12	0.103		
A-2	ppm									1641		0.02	0.016		
A-3	ppm									1667		0.02	0.011		
B-1	ppm									857			0.002		
B-2	ppm									933		0.01	0.006		
B-3	ppm								0.021	1011		1.69	0.103		

Notes: cps, count per second; ppm, parts per million

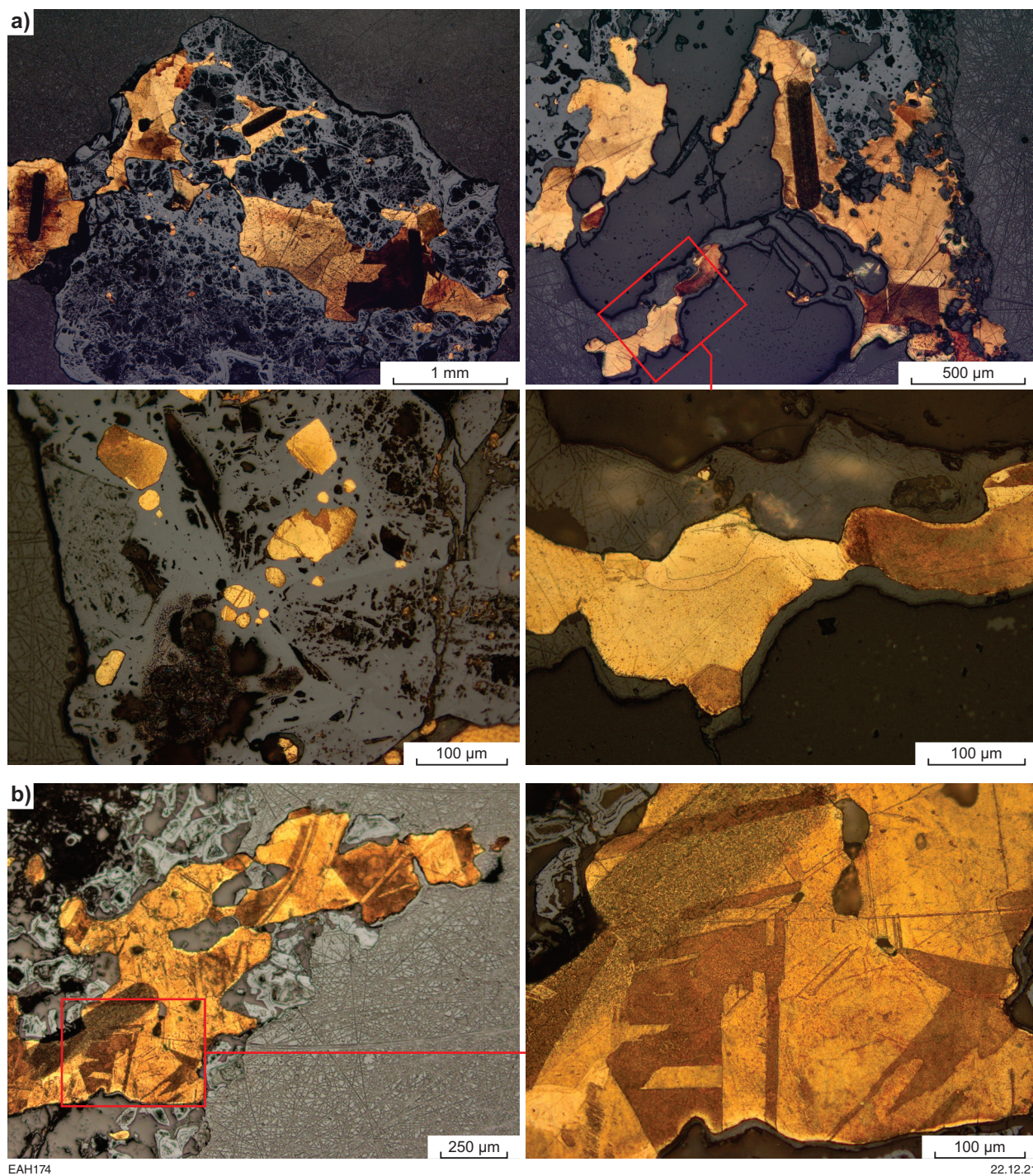


Figure 5. Reflected-light photomicrographs, after repolishing and acid etching, of parts of sample 201971: gold-bearing grains, Hillside gold prospect: a) specimen A; b) specimen B. Dark elongate lines are laser ablation tracks produced during LA-ICP-MS analyses

References

- Bagas, L, Van Kranendonk, MJ and Pawley, M 2004, Geology of the Split Rock 1:100 000 sheet: Geological Survey of Western Australia, 1:100 000 Geological Series Explanatory Notes, 43p.
- Ferguson, KM and Ruddock, I 2001, Mineral occurrences and exploration potential of the east Pilbara: Geological Survey of Western Australia, Report 81, 114p.
- Geological Survey of Western Australia 2014, Pilbara, 2014: Geological Survey of Western Australia, Geological Information Series.
- Hancock, EA and Beardsmore, TJ 2020, Provenance fingerprinting of gold from the Kurnalpi Goldfield: Geological Survey of Western Australia, Report 212, 21p.
- Hancock, EA, Blay, OA and Beardsmore, TJ 2022, 201970: gold-bearing grains, Hillside gold prospect; GSWA Mineralogy Record 4: Geological Survey of Western Australia, 9p.
- Hickman, AH 2013, Split Rock, WA Sheet 2854 (Second Edition): Geological Survey of Western Australia, 1:100 000 Geological Series.
- Hickman, AH 2021a, East Pilbara Craton: a record of one billion years in the growth of Archean continental crust: Geological Survey of Western Australia, Report 143, 187p.
- Hickman, AH 2021b, Euro Basalt (A-KEe-b): Geological Survey of Western Australia, WA Geology Online, Explanatory Notes extract, viewed 28 March 2022, <www.dmirs.gov.au/ens>.
- Hickman, AH 2021c, Kelly Group (A-KE-xb-f): Geological Survey of Western Australia, WA Geology Online, Explanatory Notes extract, viewed 28 March 2022, <www.dmirs.gov.au/ens>.
- Murray, S 2009, LBMA certified reference materials. Gold project final update: The London Bullion Market Association, Alchemist, no. 55, p. 11–12.

Recommended reference for this publication

- Hancock, EA, Blay, OA and Beardsmore, TJ 2022, 201971: gold-bearing grains, Hillside gold prospect; GSWA Mineralogy Record 5: Geological Survey of Western Australia, 8p.